Ultrafast Time-Resolved Spectroscopy of Self-Assembled Cyclic Fe(II)-Bisterpyridine Complexes

ARTICLE *in* THE JOURNAL OF PHYSICAL CHEMISTRY B · SEPTEMBER 2010

Impact Factor: 3.3 · DOI: 10.1021/jp104836k · Source: PubMed

5 AUTHORS, INCLUDING:

Zin Yoon
University of Colorado Boulder
55 PUBLICATIONS **2,091** CITATIONS
SEE PROFILE

George Richard Newkome
University of Akron
499 PUBLICATIONS **12,920** CITATIONS
SEE PROFILE

Ultrafast Time-Resolved Spectroscopy of Self-Assembled Cyclic Fe(II)−Bisterpyridine Complexes

Zin Seok Yoon,[†] Yi-Tsu Chan,[‡] Sinan Li,[‡] George R. Newkome,[‡] and Theodore Goodson III*,[†]

Department of Chemistry, University of Michigan, Ann Arbor, Michigan 48109, and Department of Chemistry, University of Akron, Akron, Ohio 44325

Received: May 27, 2010; Revised Manuscript Received: August 4, 2010

Femtosecond time-resolved absorption spectroscopy has been used to study the excited-state charge transfer dynamics in a set of self-assembled cyclic Fe(II)−bisterpyridine compounds with different π-conjugated ligands. By analyzing the dynamics, the internal conversion process involving a ligand-centered $\pi-\pi^*$ state to a lower lying metal-to-ligand charge transfer (MLCT) state was investigated. This is followed by intersystem crossing to the lowest MLCT state, which was found to occur at the ∼100 fs time scale. Vibrational cooling in the lowest MLCT state was found to occur on the 10s of femtoseconds time scale. The lowest MLCT state had an excited-state lifetime longer than 5 ns, indicating the possibility of light-induced excited-state spin trapping (LIESST).

1. Introduction

Fe(II)−ligand compounds play important roles in various biological systems, such as in hemoglobin for oxygen delivery and in ribonucleotide reductase for catalysis.[1−3] In many cases, the Fe(II)−ligand unit functions at the active site of many important biological processes. Due to their rich natural abundance, Fe(II)−containing compounds also have been studied with the idea of applying their properties to light-harvesting photosensitizer materials in the solar cell system.[4] One of the most interesting features of Fe(II)−ligand complexes might be a spin crossover (SCO) behavior. This is the process of changing the spin state from low-spin (LS) to high-spin (HS) state, or vice versa, and is induced by external perturbations such as temperature, pressure, and electromagnetic field.[5−9] Observed first by Cambi et al.[6] in a temperature-dependent study of magnetism in Fe(III)−dithiocarbamate complexes, various investigations have been performed with numerous review articles and book chapters, describing transition metal ion complexes with d^4-d^7 electronic configurations.[7−14] It was not until the 1980s that the SCO compounds were used for magneto-optic sensory devices.[15] For these practical purposes along with a basic fundamental understanding, the photophysical and magnetic properties of various types of monometallic Fe(II)− and Fe(III)−ligands compounds have been rigorously studied.

In this context, the ultrafast energy relaxation dynamics on the transition metal−ligand complexes also have been studied, focusing on SCO phenomena. McCusker and co-workers have studied the time-resolved excited-state dynamics in various Fe(II)−ligand complexes in solution.[16−20] From those reports, ultrafast deactivation of the MLCT (metal-to-ligand charge transfer) process in monomeric Fe(II)−polypyridyl compounds has been suggested. Studying both structural aspects as well as excited-state energy relaxation processes, Chergui and co-workers have recently reported the structural change of a Fe(II)−polypyridyl compound in terms of SCO process by pump−probe X-ray spectroscopy.[21−23] One of the main results in these studies is the direct observation of the Fe−N bond length change (∼0.2 Å) in the SCO process, which has been found in Fe(II)−ligand compounds.

Meanwhile, various types of self-assembled multrichromophoric metal−bisterpyridine compounds with conjugated linkers have been recently designed for their octahedral complexes with various transition metals, in order to utilize their unique photophysical features. Newkome et al. have devised cyclic multichromophoric systems with triangular,[24] pentagonal,[25] and hexagonal shapes[26] containing Fe(II) and other transition metals with different conjugated linkages.[27−30] In these molecular systems, the terpyridine derivatives have been used as ligands.[27] The tridentate 2,2′:6′,2″-terpyridine has been known to form low-spin ($t_{2g}^6e_g^0$) ground state when two terpyridine units form the coordinate bonds to one Fe(II) metal, similar to the case of low-spin ground-state compounds such as $[Fe(bpy)_3]^{2+}$ and $[Fe(phen)_3]^{2+}$.[31] The terpyridine derivatives have advantages over bipyridine complexes due to their isomeric purity and inherent linearity.[28] However, the excited-state lifetimes of Fe(II)−terpyridine complexes have been reported as being shorter than those of other metal−bipyridine complexes.[4]

With these recent developments, we investigated the photophysical properties of self-assembled Fe(II)−bisterpyridine macrocycles bearing three octahedral sphere $[FeN_6]$ moieties (Scheme 1),[30] using steady-state and femtosecond time-resolved absorption spectroscopy. The target molecular systems in Scheme 1 show three Fe(II)−bisterpyridine moieties connected with different types of π-conjugated linkers, forming hexagonal macrocycles with trimetric shapes. The excited-state relaxation processes in the current molecular systems at room temperature are discussed in terms of intersystem crossing and long-lived excited-state lifetimes. We also compare our results to recent spectroscopic studies on transition metal−ligand complexes.

2. Experimental Section

2.1. Materials. The syntheses of samples have been described previously.[30] All the measurements were carried out in

* To whom correspondence should be addressed. E-mail: tgoodson@umich.edu.
[†] University of Michigan.
[‡] University of Akron.

10.1021/jp104836k
Published on Web 08/20/2010

SCHEME 1: The Molecular Structure of Self-Assembled Fe(II)−Bisterpyridine Macrocycles Containing Three Octahedral Spheres [FeN_6] with Different Conjugated Linkages[30a]

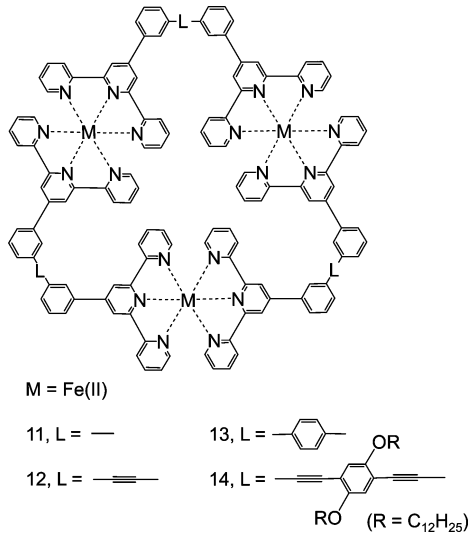

[a] The naming of molecular systems followed ref 30 for consistency.

acetonitrile (MeCN), unless stated otherwise. The naming of molecules followed that in ref 30 for consistency.

2.2. Steady-State Measurements. Ultraviolet (UV)−visible absorption spectra were recorded with an Agilent Technologies 8453 spectrophotometer. Steady-state fluorescence measurements were performed on a Fluomax-2 fluorimeter.

2.3. Femtosecond Transient Absorption Measurements. Transient absorption was used to investigate the excited-state dynamics of the samples at different excitation wavelengths and the description of the system has been provided elsewhere.[32] Briefly, the output of an amplified laser beam was split to generate pump and probe beam pulses with a beam splitter (85% and 15%). The pump beam was produced by an optical parametric amplifier (OPA-800c). The pump beams used in the present investigation were obtained from either the second or the fourth harmonic generation of the signal beam and were focused onto the sample cuvette. The probe beam was delayed with a computer controlled motion controller and then focused into a 2 mm sapphire plate to generate a white light continuum. The white light was then overlapped with the pump beam in a 1.5 mm quartz cuvette containing the sample and the change in absorbance for the signal was collected by a CCD detector (Ocean optics). Data acquisition was controlled by the software from Ultrafast Systems Inc. Typical power of the probe beam was <0.1 μJ while the pump beam was around 0.1 to 0.4 μJ per pulse. The pulse duration was obtained by fitting the solvent response, which was <130 fs. The sample was stirred with a rotating magnetic stirrer and no photodegradation of the sample has been observed before and after the pump−probe experiment.

3. Results and Discussion

3.1. Steady-State Absorption and Emission Spectra. Steady-state absorption and emission spectra of **11**−**14** were measured in MeCN (Figure 1). All four solutions in MeCN showed the purple color at room temperature, which provides evidence of the magnetic low-spin state in the ground state. The samples showed two characteristic absorption bands: $\pi-\pi^*$ transition in the 280−380 nm range, and MLCT transition (567 nm).[30] The $\pi-\pi^*$ transition bands in **11**−**14** exhibit different features,

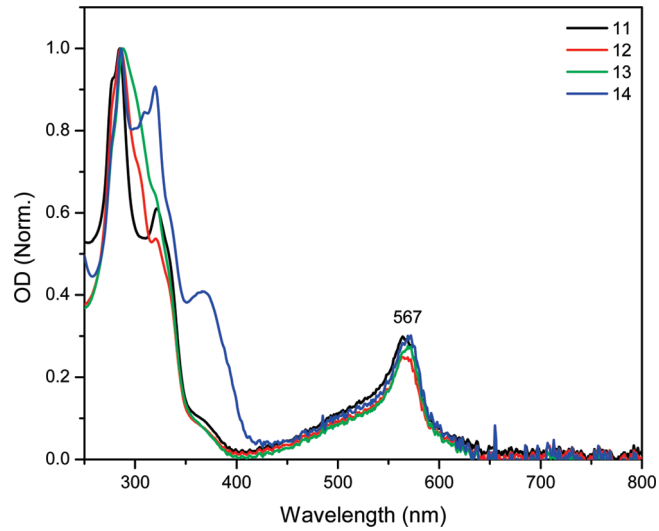

Figure 1. Normalized steady-state absorption spectra of **11**−**14** in MeCN. The absorption spectral positions around 250−400 nm are indicated in Table 1. Note that all four molecular systems show a characteristic MLCT absorption band at 567 nm.

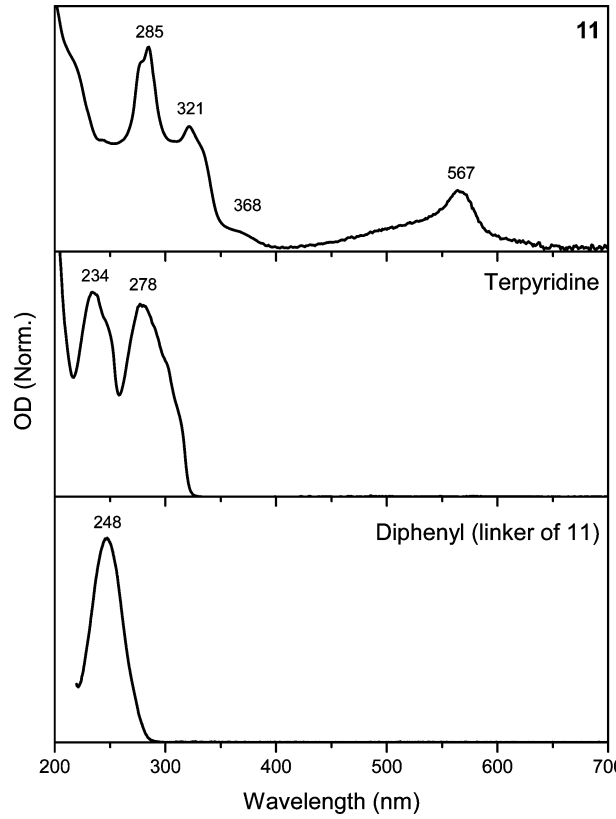

Figure 2. Steady-state absorption spectra of **11** (top) in MeCN and its ligand (terpyridine, middle) and linker (diphenyl, bottom).

reflecting the different types of π-conjugated linkers: biphenyl, diphenylacetylenyl, terphenyl, and terphenyldiacetylenyl for **11** to **14**, respectively. A distinct shoulder at 370 nm was observed in **14**, and at the same wavelength, those of **11**−**13** showed weak bands. When compared to the absorption spectra of bare 2,2′:6′,2″-terpyridine ligand[33] and biphenyl[34] linker, the absorption spectrum of **11** at the 220−380 nm range could not be reconstructed by the linear combinations of those of the bare terpyridine and the biphenyl linker (Figure 2). Thus, the broad and detailed absorption spectra in **11**−**14** compared to its

TABLE 1: Summary of Photophysical Properties of 11−14

	absorption (nm)	fluorescence (nm)	τ_1 (fs)[a]	τ_2 (ps)[a]	τ_3 (ns)[b]
11	284, 323, 371 567	387	100	9.2	>5
12	284, 323, 371 567	387,520	120	10.5	>5
13	285, 323, 371 567	399	100	9.8	>5
14	285, 320, 368 567	399	90	7.8	>5

[a] The τ_1 and τ_2 were estimated from the deconvolution fittings of the decay curves probed at 675 nm, with photoexcitation at 330 nm. [b] The τ_3 was estimated from the bleaching recovery signal at 567 nm with 330 nm pump beam in a 1000 ps detection window. The pump intensity in front of the sample cell (1.5 mm path length) was 0.4 μJ/pulse at 330 nm.

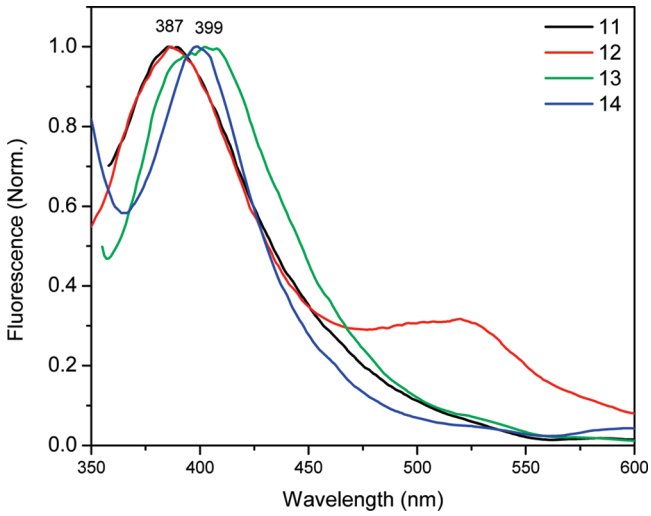

Figure 3. Steady-state fluorescence spectra of **11−14** in MeCN, where the excitation wavelengths are 330 nm. The fluorescence spectral positions are indicated in Table 1.

building units indicate the electronic interaction between Fe(II)−terpyridine ligand and π-conjugated linkers.

The fluorescence spectra of **11−14** in MeCN were monitored with the excitations at 330 nm (Figure 3). In comparison to the building blocks and terpyridine units, the fluorescence spectra from **11−14** showed broad and red-shifted features. Due to an increase in this π-conjugation length of ligands, **13** and **14** showed a red-shifted emission band compared to **11** and **12**. When monitored at 500−800 nm, however, the emission intensity was very weak, indicating that the fluorescence was quenched by the Fe(II)−bisterpyridine moieties.[20] Therefore, after photoexcitation of the $\pi-\pi^*$ transition around 300−400 nm, at least two kinds of depopulation processes can be considered, the energy transfer from the higher excited state ($\pi-\pi^*$ transition) to the lower state (MLCT) and the radiative internal conversion to the ground state. On the basis of the broad absorption spectra in the UV−vis region and the emission spectra around 360−450 nm with quenched fluorescence below 570 nm, we consider that the Fe(II) metal can play an important role. For example, it can act as a barrier that blocks the through bond energy transfer between linkers and also a structural bridge between linkages in the self-assembled system.

3.2. Femtosecond Transient Absorption Spectra and Decay Profiles. The spectroscopic characterization of multichromophoric MLCT systems provides fundamental information on the electronic energy structure that may be applied to molecular photonic/electronic devices. Due to their low fluorescence quantum yields at room temperature, the excited-state photophysical properties of **11−14** can be properly characterized by ultrafast time-resolved absorption spectroscopy. Thus, we performed femtosecond transient absorption experiments in order to reveal the excited-state energy structure and MLCT dynamics depending on the size of the π-conjugated linkages. We could accomplish this by controlling the excitation energies close to the ligand-centered $\pi-\pi^*$ transition state. As can be expected from the molecular structure and steady-state absorption spectra, there are three iso-energetic Fe(II)−bisterpyridine moieties and also iso-energetic linker units in each sample. Therefore, by photoexcitation of the ligand-centered $\pi-\pi^*$ transition state or by direct photoexcitation of the Fe(II)−bisterpyridine MLCT transition state, we may be able to observe an intra/intermolecular charge transfer process, which is possibly followed by interactions among degenerate MLCT units.

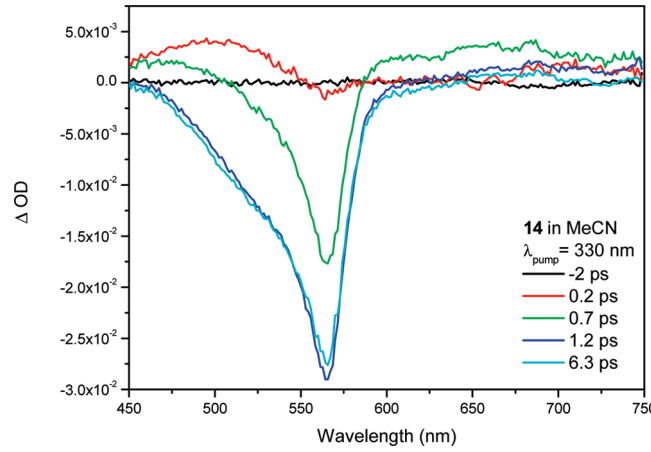

Figure 4. Femtosecond transient absorption spectra of **14** in MeCN with different time delays at room temperature, where the excitation wavelength is 330 nm.

Initially, we measured the femtosecond transient absorption spectra and decay kinetics with 330 nm excitation, in order to observe the π-conjugated linkage effect on MLCT excited-state dynamics. In Figure 4, we present the femtosecond transient absorption spectra of **14** in MeCN solvent. The ground-state bleaching signals centered at 567 nm match well with the inverted spectral profiles of the steady-state absorption. In blue and red sides of the ground-state bleaching band, broad excited-state absorption (ESA) signals were observed. The positive ΔA signals at 485 nm quickly change into negative values due to competition with the ground-state bleaching signal. However, the ESA signals of 675 nm remain as positive values, showing multiexponential decay kinetics. By deconvolution fitting, the ESA signals exhibit triple exponential decays with ~100 fs, a few picoseconds, and a nanosecond time constants (Figures 5 and 6). The femtosecond and the picosecond time components are in the range of 90−120 fs and 7.8−10.5 ps, respectively (Table 1). In addition, the longest time components (longer than 5 ns) were observed in all samples.

With 330 nm excitation experiments, we observed the transient absorption spectra and decay kinetics which showed the time constants in a wide range of time scales from femtosecond to nanosecond. The time-resolved transient spectra showed similar spectral position and bandwidth for the samples measured. Due to the weak interaction between three iso-energetic MLCT units (or perhaps due to the ultrafast internal conversion or intersystem crossing processes) there was a very small dependence of the dynamics with ligand conjugation length for this excitation regime. Thus, in order to avoid the

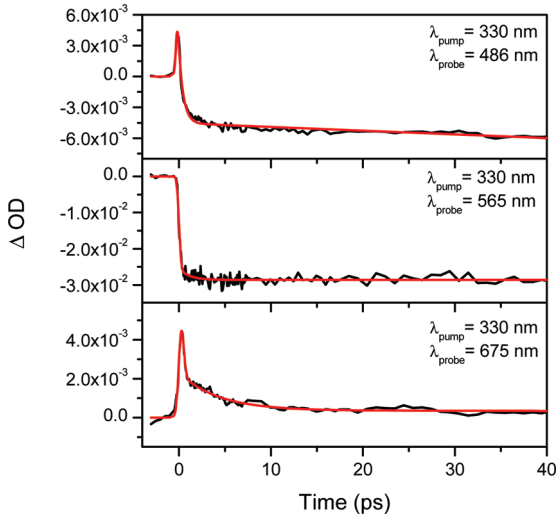

Figure 5. The femtosecond transient absorption decay profiles of **14** in MeCN, where the excitation wavelength is 330 nm.

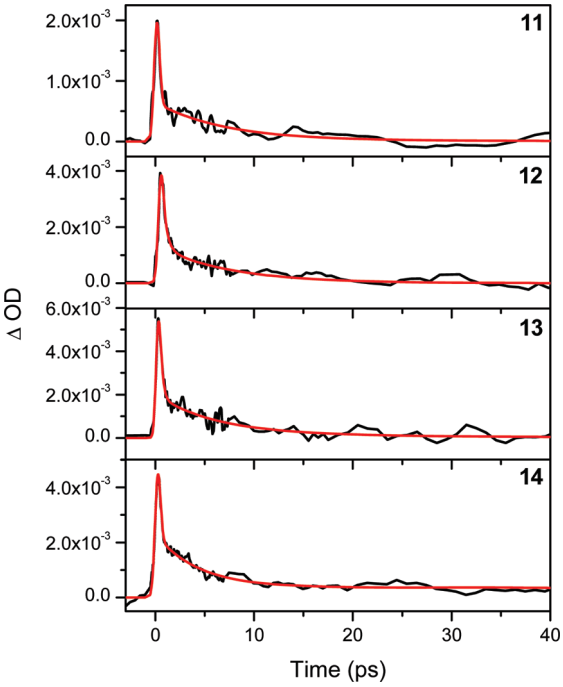

Figure 6. The temporal profiles of excited-state absorption of **11**−**14** (from top to bottom) in MeCN, where the excitation wavelength is 330 nm, and the probe wavelength is 675 nm.

involvement of the population relaxation process from ligand-centered $\pi-\pi^*$ to ^{1}MLCT state, we performed the experiment with the direct excitation of MLCT transition, using 554 and 572 nm (Figure 7). As a result, the GB signals centered at 567 nm accompanied by the ESA bands in both sides were observed, similar to previous experiments of 330 nm excitation. The excited-state decay profiles can also be fitted with a triple exponential decay function, exhibiting femto-, pico-, and nanosecond time components (see Table 1).

With both 330 and 567 nm excitation experiments, we have measured the excited-state time constant over a wide range of time scales. To understand the femto-, pico-, and nanosecond time constants corresponding to the excited-state relaxation processes in **11**−**14**, we need to examine the previously reported ultrafast studies on metal−ligand complexes. The analogous ultrafast decay kinetics can be found in the previous case of monometalated $[Fe(tren(py)_3)](PF_6)_2$, showing ∼300 fs and 8

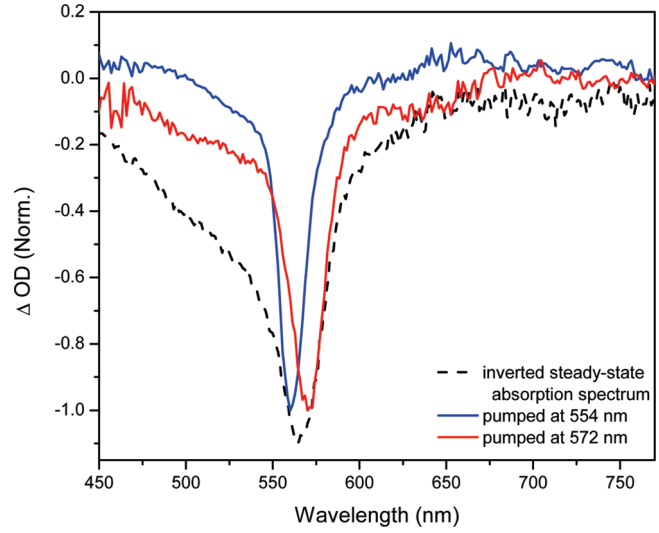

Figure 7. Femtosecond transient absorption spectra of **12** in MeCN, with 554 and 572 nm excitation, compared to the inverted steady-state absorption spectrum (dotted line).

± 3 ps time constants reported by McCusker et al.[35] Using femtosecond and nanosecond time-resolved spectroscopy, they assigned the femtosecond time constant as the ultrafast intersystem crossing from ^{1}MLCT to ^{3}MLCT and the picosecond component as the vibrational cooling process in the lowest excited triplet MLCT state. An important conclusion in this ultrafast spectroscopic study was that a spin-forbidden intersystem crossing, conventionally known as a comparatively slower process, can also occur in the femtosecond time scale in Fe(II)−metal containing MLCT molecular systems. They explained the reasons of this fast intersystem crossing would be the spin−orbit coupling by transition metal and the larger Franck−Condon overlap associated with geometric distortion. In a recent ultrafast time-resolved X-ray spectroscopic study by Chergui et al.,[21] the photoinduced SCO from low-spin ground state ($^1A_1$) to high-spin excited state ($^5T_2$) has been observed on the Fe(II)−polypyridyl complex. When excited into the ^{1}MLCT state, they assigned that the population relaxation occurs with a two-step intersystem crossing process: ^{1}MLCT → ^{3}MLCT → ^{5}T. From the observed relaxation dynamics, it can be inferred that the ligand field strength is diminished by the elongation of the Fe−N bond length, resulting in the smaller band splitting energy between t_{2g} and e_g atomic d-orbitals in one Fe(II)−bisterpyridine moiety. In addition, Bhasikuttan et al. have also reported the ultrafast decay in $[Ru(bpy)_3]^{2+}$ by fluorescence up-conversion study, exhibiting an ∼40 fs time constant.[36] Similar to the previous $[Fe(tren(py)_3)](PF_6)_2$ case, the ultrafast intersystem crossing from excited ^{1}MLCT states to vibrationally hot triplet manifold was indicated as an origin for the ultrafast process.

On the basis of these previous assignments of ultrafast processes, we examined our experimental results to assign the excited-state photophysical properties of **11**−**14**. Among the three different ranges of time constants in our study, the first result we considered as a notable finding is the fastest time constants, which are in 90−120 fs for the different structures. In previous studies of MLCT complexes, the femtosecond components were assigned as an intersystem crossing from ^{1}MLCT to ^{3}MLCT, but in our case, it is clear that the femtosecond time constants exhibit not only the ultrafast intersystem crossing from ^{1}MLCT to ^{3}MLCT, but also the internal conversion from LC $\pi-\pi^*$ state to ^{1}MLCT. This is

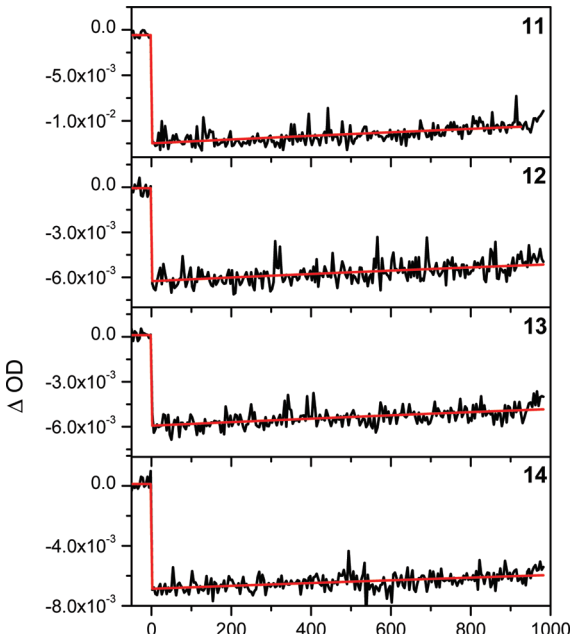

Figure 8. The femtosecond transient absorption decay profiles of **11**−**14** in MeCN, monitored at 520 nm, after photoexcitation at 554 nm.

because for the different excitation experiments of 330 and 567 nm, where the possibility of internal conversion could have been excluded in the latter case, the two excitation regimes exhibited similar results. Similar to this case, Gustafson et al.[36] also reported in the ultrafast spectroscopic study on $Mo_2(O_2C\text{-}9\text{-}anthracene)_4$ that the transient absorption spectra and decay kinetics by 347 and 514.5 nm excitation experiments are similar, which indicates the ultrafast internal conversion from ligand-centered to ^{1}MLCT state.[37]

In Figure 8, we present the decay profiles of femtosecond transient absorption of **11**−**14** in MeCN with the excitation at 554 nm, corresponding to direct excitation to the ^{1}MLCT state. According to the excited-state deactivation mechanism suggested in previous studies, it is possible to explain the nanosecond decay components of ∼5 ns as a result of a spin crossover in terms of light-induced excited spin state trapping (LIESST), which was first observed by McGarvey in solution.[38] As described in the Introduction, Fe(II)−metal based complexes have attracted much interest for the photomagnetic applications, and the excited-state lifetime is one of the critical characteristics for this application. In the complexes studied here we can see that the lifetimes are of the desired time scale for this important application as well. LIESST has been reported in various Fe−ligand SCO materials and the slow excited-state population decay is a qualitative index of LIESST, because it is induced by the spin-forbidden intersystem crossing from high-spin excited state to low-spin ground state via thermal tunneling.

On the basis of our time-resolved experimental results, we can summarize the excited-state dynamics in **11**−**14** in Scheme 2. After the initial photoexcitation, an ultrafast internal conversion occurs within a few hundred femtosecond time scale, followed by an ultrafast intersystem crossing to the ^{3}MLCT state. After a vibrational cooling process, the excited-state population remains in the metastable excited state longer than >5 ns. The excited-state dynamics in our multichromophoric systems is similar to those of monomeric cases. This might infer that the initial excitation energy is localized in a single Fe(II)−bisterpyridine MLCT unit, because all the spectroscopic results in the four samples showed a similar excited-state dynamics, acting

SCHEME 2: Energy and Charge Transfer Scheme (left) and Excited-State Energy Relaxation Diagram (right) in Self-Assembled Hexagonal Fe(II)−Bisterpyridine Complexes[a]

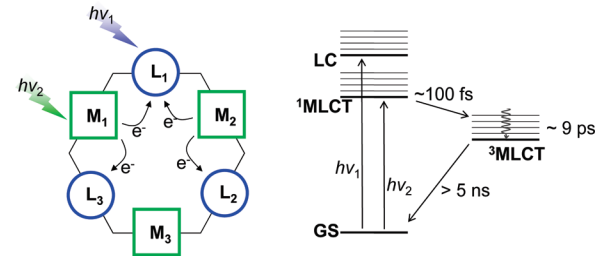

[a] $h\nu_1$: excitation energy for ligand-centered (LC) $\pi-\pi^*$ state. $h\nu_2$: energy for MLCT (metal-to-ligand charge transfer).

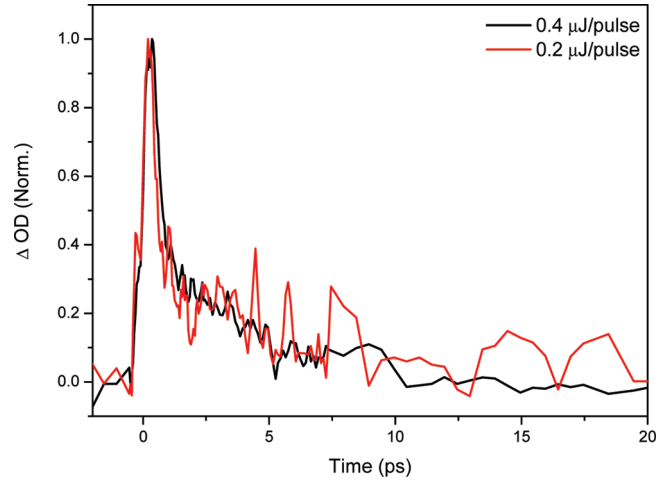

Figure 9. Normalized femtosecond transient absorption decay profiles of **11** at high (0.4 μJ/pulse, black) and low (0.2 μJ/pulse, red) incident intensities of photoexcitation at 330 nm, monitored at 675 nm.

like a monomeric unit. This localized excitation between MLCT units is reminiscent of the weak cooperativity of other Fe(II)−ligand complexes in the solid state.[39] In addition to this, we have performed the pump-intensity dependent transient absorption experiment (Figure 9) in order to probe the possible interaction between the MLCT units. As seen in Figure 9, for **11** as an example, the difference between high- and low-intensity excitation in decay profiles was not significantly observed, exhibiting linear dependence on excitation power. This result suggests the possibility of localized excitation.

4. Conclusions

The photophysical properties of the self-assembled cyclic Fe(II)−bisterpyridine complexes with different linkers were investigated by steady-state and femtosecond time-resolved absorption spectroscopy. The broad absorption spectra in the $\pi-\pi^*$ transition region indicate the strong electronic interaction between MLCT units and linker moieties. By ultrafast pump−probe transient absorption spectroscopy, we found that the excited-state energy transfer occurs from ligand−linker moieties to Fe(II)−bisterpyridine moieties, judging from the direct excitation on the $\pi-\pi^*$ state, followed by ultrafast intersystem crossing and the relaxation in the lowest excited state. The time constant in the lowest excited state showed a few nanoseconds, which can be observed in the previous cases in terms of light-induced excited spin-state trap (LIESST) effect.

Acknowledgment. This work was supported by the National Science Foundation (Polymers, Materials, DMR) and through

a fellowship by the National Research Foundation of Korea Grant funded by the Korean Government [NRF-2009-352-C00053].

References and Notes

(1) Lukin, J. A.; Ho, C. *Chem. Rev.* **2004**, *104*, 1219–1230.

(2) Stubbe, J.; Nocera, D. G.; Yee, C. S.; Chang, M. C. Y. *Chem. Rev.* **2003**, *103*, 2167–2202.

(3) Thelander, L. *Nat. Genet.* **2007**, *39*, 703–704.

(4) Brady, C.; McGarvey, J. J.; McCusker, J. K.; Toftlund, H.; Hendrickson, D. N. *Top. Curr. Chem.* **2004**, *235*, 1–22.

(5) Gütlich, R.; Goodwin, H. A. *Top. Curr. Chem.* **2004**, *233*, 1–47, and references cited therein.

(6) Cambi, L.; Cagnasso, A. *Atti Accad. Naz. Lincei* **1931**, *13*, 809.

(7) Garcia, Y.; Gütlich, P. *Top. Curr. Chem.* **2004**, *234*, 49–62.

(8) Weber, B.; Kaps, E. S.; Obel, J.; Achterhold, K.; Parak, F. G. *Inorg. Chem.* **2008**, *47*, 10779–10787.

(9) Konig, E.; Ritter, G.; Kulshreshtha, S. K. *Chem. Rev.* **1985**, *85*, 219–234.

(10) Gütlich, P.; Garcia, Y.; Goodwin, H. A. *Chem. Soc. Rev.* **2000**, *29*, 419–427.

(11) Gütlich, P.; Hauser, A.; Spiering, H. *Angew. Chem., Int. Ed. Engl.* **1994**, *33*, 2024–2054.

(12) Nihei, M.; Shiga, T.; Maeda, Y.; Oshio, H. *Coord. Chem. Rev.* **2007**, *251*, 2606–2621.

(13) Hauser, A. *Top. Curr. Chem.* **2004**, *234*, 155–198.

(14) Real, J. A.; Gaspar, A. B.; Niel, V.; Munoz, M. C. *Coord. Chem. Rev.* **2003**, *236*, 121–141.

(15) Sato, O. *Acc. Chem. Res.* **2003**, *36*, 692–700.

(16) Smeigh, A. L.; Creelman, M.; Mathies, R. A.; McCusker, J. K. *J. Am. Chem. Soc.* **2008**, *130*, 14105–14107.

(17) Juban, E. A.; Smeigh, A. L.; Monat, J. E.; McCusker, J. K. *Coord. Chem. Rev.* **2006**, *250*, 1783–1791.

(18) Yeh, A. T.; Shank, C. V.; McCusker, J. K. *Science* **2000**, *289*, 935–938.

(19) Weldon, B. T.; Wheeler, D. E.; Kirby, J. P.; McCusker, J. K. *Inorg. Chem.* **2001**, *40*, 6802–6812.

(20) McCusker, J. K.; Walda, K. N.; Dunn, R. C.; Simon, J. D.; Magde, D.; Hendrickson, D. N. *J. Am. Chem. Soc.* **1993**, *115*, 298–307.

(21) Bressler, Ch.; Milne, C.; Pham, V.-T.; ElNahhas, A.; van der Veen, R. M.; Gawelda, W. S.; Johnson, S.; Beud, P.; Grolimund, D.; Kaiser, M.; Borca, C. N.; Ingold, G.; Abela, R.; Chergui, M. *Science* **2009**, *323*, 489–492.

(22) Gawelda, W.; Cannizzo, A.; Pham, V.-T.; van Mourik, F.; Bressler, C.; Chergui, M. *J. Am. Chem. Soc.* **2007**, *129*, 8199–8206.

(23) Gawelda, W.; Pham, V.-T.; Benfatto, M.; Zaushitsyn, Y.; Kaiser, M.; Grolimund, D.; Johnson, S. L.; Abela, R.; Hauser, A.; Bressler, C.; Chergui, M. *Phys. Rev. Lett.* **2007**, *98*, 057401.

(24) Hwang, S.-H.; Moorefield, C. N.; Fronczek, F. R.; Lukoyanova, O.; Echegoyen, L.; Newkome, G. R. *Chem. Commun.* **2005**, 713–715.

(25) Hwang, S.-H.; Wang, P.; Moorefield, C. N.; Godínez, L. A.; Manríquez, J.; Bustos, E.; Newkome, G. R. *Chem. Commun.* **2005**, 4672–4674.

(26) Hwang, S.-H.; Moorefield, C. N.; Wang, P.; Fronczek, F. R.; Courtney, B. H.; Newkome, G. R. *Dalton Trans.* **2006**, 3518–3522.

(27) Eryazici, I.; Moorefield, C. N.; Newkome, G. R. *Chem. Rev.* **2008**, *108*, 1834–1895.

(28) Schubert, U. S.; Hofmeier, H.; Newkome, G. R. *Modern Terpyridine Chemistry*; Wiley-VCH: Weinheim, Germany, 2006.

(29) Newkome, G. R.; Wang, P.; Moorefield, C. N.; Cho, T. J.; Mohapatra, P. P.; Sinan Li, S.; Hwang, S.-H.; Lukoyanova, O.; Echegoyen, L.; Palagallo, J. A.; Iancu, V.; Hla, S.-W. *Science* **2006**, *312*, 1782–1785.

(30) Li, S.; Moorefield, C. N.; Wang, P.; Shreiner, C. D.; Newkome, G. R. *Eur. J. Org. Chem.* **2008**, 3328–3334.

(31) Daku, L. M. L.; Hauser, A. *J. Phys. Chem. Lett.* **2010**, *1*, 1830–1835.

(32) Ramakrishna, G.; Bhaskar, A.; Goodson, T., III. *J. Phys. Chem. B* **2006**, *110*, 20872–20878.

(33) The steady-state absorption spectrum of 2,2′:6′,2″-terpyridine was measured in MeCN solvent.

(34) Gomes, P. J. S.; Serpa, C; Arnaut, L. G. *J. Photochem. Photobiol. A* **2006**, *184*, 228–233.

(35) Monat, J. E.; McCusker, J. K. *J. Am. Chem. Soc.* **2000**, *122*, 4092–4097.

(36) Bhasikuttan, A. C.; Suzuki, M.; Nakashima, S.; Okada, T. *J. Am. Chem. Soc.* **2002**, *124*, 8398–8405.

(37) Burdzinski, G. T.; Ramnauth, R.; Chisholm, M. H.; Gustafson, T. L. *J. Am. Chem. Soc.* **2006**, *128*, 6776–6777.

(38) McGarvey, J.; Lawthers, I. *J. Chem. Soc., Chem. Commun.* **1982**, 906.

(39) Nakamoto, T.; Tan, Z.-C.; Sorai, M. *Inorg. Chem.* **2001**, *40*, 3805–3809.

JP104836K